# The Minimal $CO_2$-Concentrating Mechanism of *Prochlorococcus* spp. MED4 Is Effective and Efficient[1][W][OPEN]

**Brian M. Hopkinson*, Jodi N. Young, Anna L. Tansik, and Brian J. Binder**

Department of Marine Sciences, University of Georgia, Athens, Georgia 30602 (B.M.H., A.L.T., B.J.B.); and Department of Geosciences, Princeton University, Princeton, New Jersey 08544 (J.N.Y.)

**ORCID ID: 0000-0002-0844-0794 (B.M.H.).**

As an oligotrophic specialist, *Prochlorococcus* spp. has streamlined its genome and metabolism including the $CO_2$-concentrating mechanism (CCM), which serves to elevate the $CO_2$ concentration around Rubisco. The genomes of *Prochlorococcus* spp. indicate that they have a simple CCM composed of one or two $HCO_3^-$ pumps and a carboxysome, but its functionality has not been examined. Here, we show that the CCM of *Prochlorococcus* spp. is effective and efficient, transporting only two molecules of $HCO_3^-$ per molecule of $CO_2$ fixed. A mechanistic, numerical model with a structure based on the CCM components present in the genome is able to match data on photosynthesis, $CO_2$ efflux, and the intracellular inorganic carbon pool. The model requires the carboxysome shell to be a major barrier to $CO_2$ efflux and shows that excess Rubisco capacity is critical to attaining a high-affinity CCM without $CO_2$ recovery mechanisms or high-affinity $HCO_3^-$ transporters. No differences in CCM physiology or gene expression were observed when *Prochlorococcus* spp. was fully acclimated to high-$CO_2$ (1,000 $\mu$L $L^{-1}$) or low-$CO_2$ (150 $\mu$L $L^{-1}$) conditions. *Prochlorococcus* spp. CCM components in the Global Ocean Survey metagenomes were very similar to those in the genomes of cultivated strains, indicating that the CCM in environmental populations is similar to that of cultured representatives.

The marine picocyanobacteria genus *Prochlorococcus* along with its sister group the marine genus *Synechococcus* dominate primary production in oligotrophic marine environments (Partensky et al., 1999). *Prochlorococcus* spp. is an oligotrophic specialist with several key adaptations allowing it to outcompete other phytoplankton in the stable, low-nutrient regions where it thrives. These adaptations include small cell size (less than 1 $\mu$m), allowing it to effectively capture nutrients and light, and genome streamlining, which minimizes nutrient requirements (Partensky and Garczarek, 2010). At approximately 1,900 genes, the genomes of high-light-adapted *Prochlorococcus* spp. are the smallest known among photoautotrophs, suggesting that this is about the minimum number of genes needed to make a cell from inorganic constituents and light (Rocap et al., 2003). Genome reduction has been accomplished by both the loss of entire pathways and complexes, such as the phycobilisomes and many regulatory capabilities, and the paring down of systems to their minimal components, as is the case for the circadian clock and the photosynthetic complexes (Rocap et al., 2003; Kettler et al., 2007; Partensky and Garczarek, 2010).

As part of this genome streamlining, the $CO_2$-concentrating mechanism (CCM), which enhances the efficiency of photosynthesis by elevating the concentration of $CO_2$ around Rubisco, has been reduced to what appears to be the minimal number of components necessary for a functional CCM (Badger and Price, 2003; Badger et al., 2006). In typical cyanobacteria, the CCM is composed of $HCO_3^-$ transporters, $CO_2$ uptake systems, and the carboxysome, a protein microcompartment in which Rubisco and carbonic anhydrase (CA) are enclosed. $HCO_3^-$ is accumulated in the cytoplasm by direct import from the environment and by the active conversion of $CO_2$ to $HCO_3^-$ via an NADH-dependent process, which constitutes the $CO_2$ uptake mechanism (Shibata et al., 2001). The accumulated $HCO_3^-$ then diffuses into the carboxysome, where CA converts it to $CO_2$, elevating the concentration of $CO_2$ around Rubisco (Reinhold et al., 1987; Price and Badger, 1989).

Whereas some cyanobacteria have up to three different families of $HCO_3^-$ transporters with differing affinities for use under different environmental conditions, *Prochlorococcus* spp. has only one or two families (Badger et al., 2006). Most cyanobacteria have low-affinity and high-affinity $CO_2$ uptake systems, but no $CO_2$ uptake systems are apparent in *Prochlorococcus* spp. genomes. The carboxysome of *Prochlorococcus* spp. and other $\alpha$-cyanobacteria has apparently been laterally transferred from chemoautotrophs, but all of the required components of the carboxysome are present and it is

[1] This work was supported by the National Science Foundation (grant nos. EF 1041023 and MCB 1129326).

* Address correspondence to bmhopkin@uga.edu.

The author responsible for distribution of materials integral to the findings presented in this article in accordance with the policy described in the Instructions for Authors (www.plantphysiol.org) is: Brian M. Hopkinson (bmhopkin@uga.edu).

[W] The online version of this article contains Web-only data.

[OPEN] Articles can be viewed online without a subscription.

www.plantphysiol.org/cgi/doi/10.1104/pp.114.247049

  

functional (Badger et al., 2002; Roberts et al., 2012). Despite its simplicity, this CCM is likely functional. $HCO_3^-$ can be accumulated in the cytoplasm by the $HCO_3^-$ transporters and then diffuse into the carboxysome for conversion to $CO_2$ and subsequent fixation by Rubisco. However, the functionality of the CCM in *Prochlorococcus* spp. has not yet been tested. *Prochlorococcus* spp. is a representative of the $\alpha$-cyanobacteria, a group with distinct CCMs, which have been much less well studied than the CCMs of $\beta$-cyanobacteria (Rae et al., 2011, 2013; Whitehead et al., 2014).

We characterized inorganic carbon ($C_i$) acquisition and processing in *Prochlorococcus* spp. MED4, examined the effect of long-term acclimation to different $CO_2$ concentrations on CCM physiology and gene expression, and searched metagenomes for *Prochlorococcus* spp. CCM genes to determine if CCMs in the natural populations are similar to cultured strains.

## RESULTS

### Photosynthesis and $C_i$ Uptake versus $C_i$

Rates of net photosynthesis, $CO_2$ flux, and $HCO_3^-$ flux were measured as $C_i$ was gradually supplied to *Prochlorococcus* spp. MED4 acclimated to 150 and 1,000 $\mu$L $L^{-1}$ $CO_2$. The net photosynthesis and $HCO_3^-$ flux data were fit with Michaelis-Menten functions to summarize the data (Fig. 1). Net photosynthetic rates began to decline slightly above approximately 1 mM $C_i$, most likely due to extended time in the assay chamber, so these data were excluded from the fits. The one-half-saturation constant of net photosynthesis for inorganic carbon ($K_P$) was low (approximately 30 $\mu$M $C_i$) and unaffected by culture $CO_2$ concentration (Fig. 1; Table I; 95% confidence intervals overlap based on SE in the fit). Maximal photosynthetic rates ($P_{max}$) were also not significantly different between the $CO_2$ treatments. The one-half-saturation constant of $HCO_3^-$ uptake for inorganic carbon ($K_B$) was significantly higher than $K_P$ (95% confidence intervals do not overlap), but neither $K_B$ nor the maximal $HCO_3^-$ uptake rate ($B_{max}$) was significantly different between $CO_2$ treatments. Net growth rates were not affected by $CO_2$ (150 $\mu$L $L^{-1}$ $CO_2$, 0.37 ± 0.05 $d^{-1}$; 1,000 $\mu$L $L^{-1}$ $CO_2$, 0.36 ± 0.01 $d^{-1}$).

$CO_2$ concentrations increased above equilibrium during photosynthesis, except at low $C_i$ concentrations (200 $\mu$M or less), indicating $CO_2$ efflux from *Prochlorococcus* spp. rather than $CO_2$ uptake. We verified that $CO_2$ was above equilibrium concentrations by adding bovine CA, which led to a rapid decline in the $CO_2$ concentration to equilibrium levels (Fig. 2A). In a separate experiment, $^{13}C^{18}O$-labeled $C_i$ was added as the $C_i$ source. During photosynthesis, an increase in $^{13}C^{16}O^{16}O$ was observed, which indicates that the $CO_2$ originates from $C_i$ taken up for photosynthesis rather than respiratory $^{12}CO_2$ and that the $C_i$ has undergone many hydration/dehydration cycles leading to the removal of the $^{18}O$ label. $CO_2$ fluxes were near zero at low $C_i$ (200 $\mu$M or less) but became negative (representing net $CO_2$ efflux) beyond that, reaching their one-half-maximal level at approximately 400 to 500 $\mu$M $C_i$.

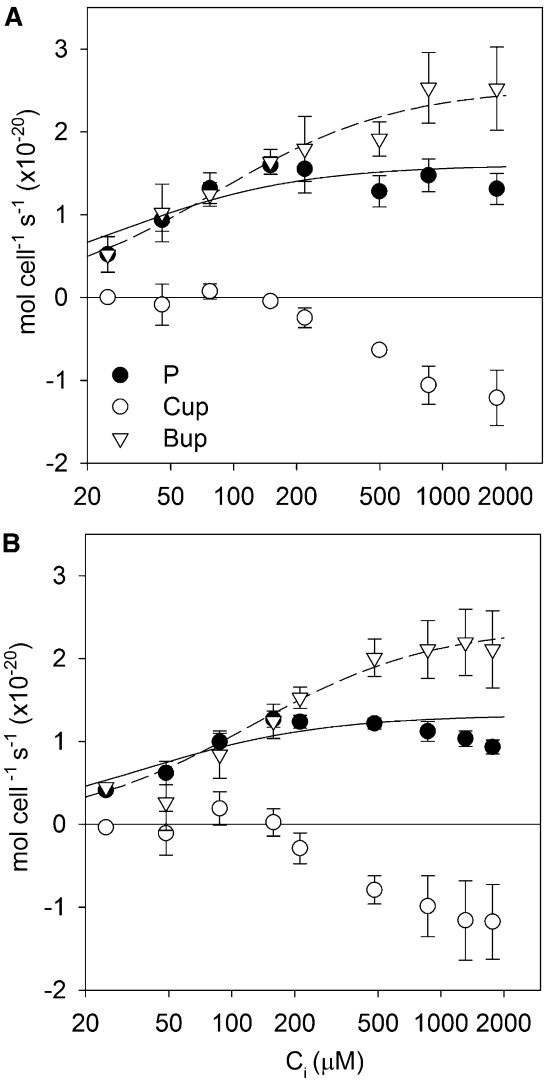


**Figure 1.** Rates of photosynthesis (P), $CO_2$ uptake or efflux (Cup), and $HCO_3^-$ uptake (Bup) in *Prochlorococcus* spp. MED4 as a function of $C_i$ concentration for cells grown at 150 $\mu$L $L^{-1}$ $CO_2$ (A) and 1,000 $\mu$L $L^{-1}$ $CO_2$ (B). Positive rates indicate uptake into the cell, and negative rates indicate efflux from the cell. $C_i$ concentrations in the culture medium were approximately 1,850 $\mu$M at 150 $\mu$L $L^{-1}$ $CO_2$ and approximately 2,200 $\mu$M at 1,000 $\mu$L $L^{-1}$ $CO_2$.

### Intracellular $C_i$ Pools

Intracellular $C_i$ pools were estimated from the $CO_2$ efflux that occurred at the beginning of each dark cycle. These data were highly variable, and there were no significant differences between the two $CO_2$ treatments, so the data from the two treatments were pooled. The intracellular $C_i$ pool increased as the extracellular $C_i$ increased, reaching a maximal value of approximately 15 mM around 1,000 $\mu$M extracellular $C_i$ (Fig. 3A).

**Table I.** *Michaelis-Menten fits to photosynthesis and $C_i$ fluxes as a function of $C_i$ and SE values in the fitted parameters*

For the net photosynthesis fits, the data at $C_i$ greater than 1 mM were excluded from the fit.

| Parameter | 150 $\mu$L L$^{-1}$ $CO_2$ | | 1,000 $\mu$L L$^{-1}$ $CO_2$ | |
|---|---|---|---|---|
| | Fitted Value | SE | Fitted Value | SE |
| $K_P$ ($\mu$M) | 28 | 8 | 37 | 8 |
| $P_{max}$ ($\times 10^{-20}$ mol cell$^{-1}$ s$^{-1}$) | 1.60 | 0.09 | 1.32 | 0.06 |
| $K_B$ ($\mu$M) | 82 | 15 | 127 | 23 |
| $B_{max}$ ($\times 10^{-20}$ mol cell$^{-1}$ s$^{-1}$) | 2.54 | 0.12 | 2.39 | 0.12 |

Cyanobacteria typically have somewhat larger intracellular $C_i$ pools (Kaplan et al., 1980; Badger et al., 1985), but it should be noted that the calculated intracellular $C_i$ pool is highly dependent on the cell diameter used to determine the volume of the spherical cells. We used a cell diameter of 0.7 $\mu$m, most commonly reported for the MED4 strain (Bertilsson et al., 2003; Ting et al., 2007), but values as low as 0.5 $\mu$m have been used (Morris et al., 2011), which would result in 3-fold lower volume and so 3-fold higher intracellular $C_i$. A Michaelis-Menten fit to the data had a one-half-saturation constant of 550 $\pm$ 210 $\mu$M $C_i$ and a saturation value of 21 $\pm$ 3 mM. The intracellular $C_i$ pool was linearly related to the rate of $CO_2$ efflux (Fig. 3B; $r^2$ = 0.94, $P < 0.001$) but was not directly related to the net photosynthetic rate (Fig. 3C). The $CO_2$ concentration in the carboxysome was calculated from the intracellular $C_i$ concentration by assuming that the cytoplasmic pH was 7.35 (Falkner et al., 1976; Kallas and Dahlquist, 1981; Belkin et al., 1987), that the carboxysome pH is the same as that of the cytoplasm (Menon et al., 2010), and that $CO_2$ and $HCO_3^-$ are in equilibrium in the carboxysome. At seawater $C_i$ (2 mM), the internal $C_i$ pool was approximately 15 mM and the estimated $CO_2$ concentration in the carboxysome was approximately 500 $\mu$M.

### Photosynthesis and $C_i$ Uptake versus Irradiance

Rates of net photosynthesis, $CO_2$ flux, and $HCO_3^-$ flux were measured as irradiance was gradually increased on *Prochlorococcus* spp. MED4 cultures acclimated to 150 $\mu$L L$^{-1}$ $CO_2$ (Fig. 4; Table II). The net photosynthesis and $HCO_3^-$ flux data were fit with Michaelis-Menten functions allowing an offset to account for negative net photosynthesis (respiration) in the dark (zero irradiance). The one-half-saturation of net photosynthesis for irradiance ($I_k$) was 63 $\mu$mol photons m$^{-2}$ s$^{-1}$ and $P_{max}$ was 1.62 $\times$ 10$^{-20}$ mol cell$^{-1}$ s$^{-1}$. The one-half-saturation of $HCO_3^-$ uptake for irradiance ($I_B$) was 42 $\mu$mol photons m$^{-2}$ s$^{-1}$ and $B_{max}$ was 2.57 $\times$ 10$^{-20}$ mol cell$^{-1}$ s$^{-1}$. The maximal rates of net photosynthesis and $HCO_3^-$ uptake are indistinguishable from those measured in the photosynthesis versus $C_i$ experiments, showing that rates were light saturated in these experiments, which were conducted at 200 $\mu$mol photons m$^{-2}$ s$^{-1}$. Additionally, $I_k$ and $I_B$ are significantly below the incubator irradiance (100 $\mu$mol photons m$^{-2}$ s$^{-1}$), showing that these rates are light saturated, or nearly so, under growth conditions.

### Rubisco Content and Kinetics

Cellular Rubisco content as measured by quantitative western blots was 8.25 $\pm$ 0.7 $\times$ 10$^{-22}$ mol Rubisco hexadecamer cell$^{-1}$ (6.6 $\times$ 10$^{-21}$ mol active site cell$^{-1}$) at 150 $\mu$L L$^{-1}$ $CO_2$. The one-half-saturation constant of Rubisco for $CO_2$ was 263 $\pm$ 5 $\mu$M (Supplemental Fig. S1), similar to a previously measured value of 295 $\mu$M (Roberts et al., 2012). Both of these $K_m$ values come from measurements made at pH 8, and the Roberts et al. (2012) measurements were made on purified carboxysomes, whereas ours were with a crude extract

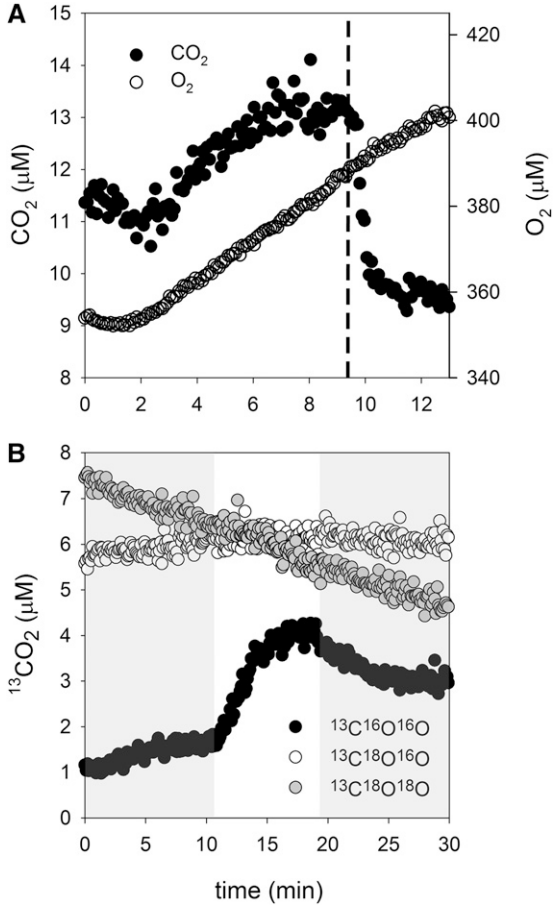


**Figure 2.** A, Sample data showing increases in $CO_2$ concentrations upon illumination in an assay chamber containing *Prochlorococcus* spp. MED4 and 2 mM $C_i$. That the $CO_2$ concentration exceeds equilibrium with $HCO_3^-$ is illustrated by the addition of bovine CA just after 9 min (dashed line), which establishes equilibrium between $CO_2$ and $HCO_3^-$. Oxygen data show that photosynthesis was not affected by the addition of bovine CA. B, A light/dark cycle with 2 mM $^{13}C^{18}O$-labeled $C_i$ added to the assay chamber (darkness = gray background; illumination at 250 $\mu$mol photons m$^{-2}$ s$^{-1}$ = white background).

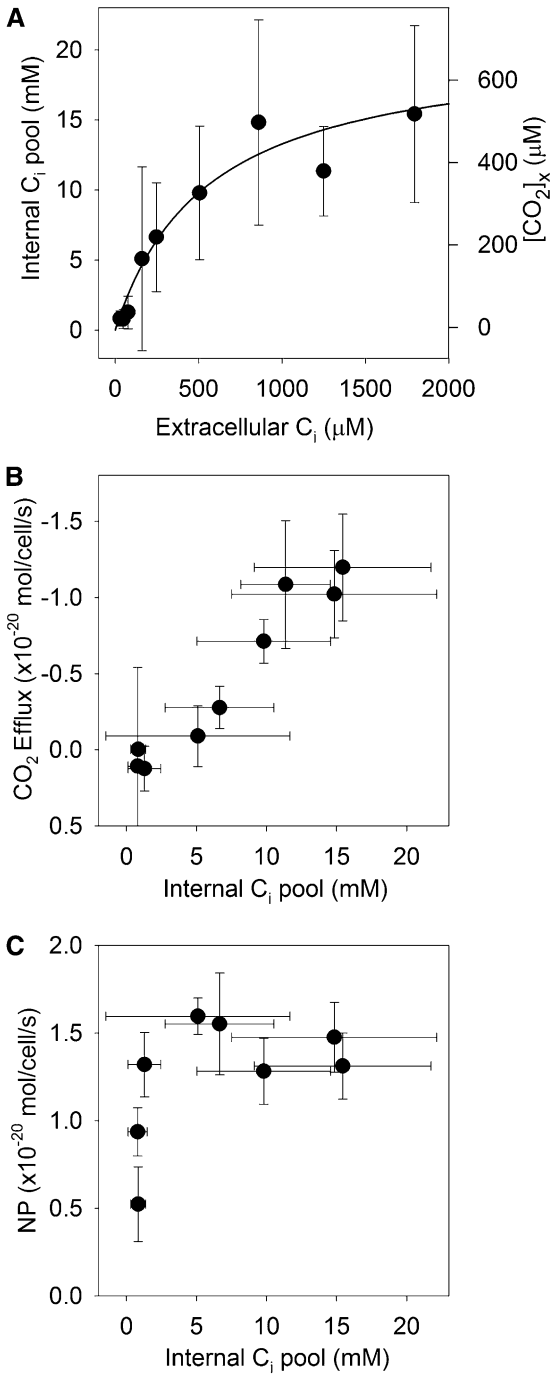


**Figure 3.** A, Intracellular $C_i$ pool as a function of external $C_i$ concentration as inferred from $CO_2$ efflux following each light phase. The $CO_2$ concentration in the carboxysome ($[CO_2]_x$) was calculated assuming that the intracellular pH is 7.35. A Michaelis-Menten fit to the data had a one-half-saturation constant of 550 ± 210 μM $C_i$ and a saturation value of 21 ± 3 mM. B, Relationship between $CO_2$ efflux and the intracellular $C_i$ pool. C, Net photosynthesis (NP) of *Prochlorococcus* spp. MED4 acclimated to 150 μL $L^{-1}$ $CO_2$ as a function of the intracellular $C_i$ pool.

that likely contained a mix of intact carboxysomes and single Rubisco molecules. They are lower than the value reported for purified *Prochlorococcus* spp. Rubisco (750 μM) by Scott et al. (2007) made at pH 7.5. These differences may be accounted for by pH, since lower pH reduces the $K_m$ of cyanobacterial Rubisco (Badger 1980), or by differences between intact carboxysomes and purified Rubisco either due to actual changes in $K_m$ of the enzyme or environmental effects. The consequences of uncertainty in $K_m$ for the CCM model are discussed below.

### Modeling

A mechanistic model of the *Prochlorococcus* spp. CCM (see "Materials and Methods") was parameterized using data obtained in this study and values from the literature (Table III; Fig. 5A). The model was used to assess our understanding of CCM structure based on its ability to match rates of photosynthesis, $CO_2$ efflux, and internal $C_i$ concentrations observed under culture conditions. While the model structure should be applicable to a broader range of environmental conditions, the specific implementation used here should not be applied without modification to more general environmental conditions, since the model was parameterized based on cultures grown under a narrow range of conditions (constant temperature, light, etc.).

The only critical parameter that has no literature constraints and was not measured in this study was the $CO_2$ transfer coefficient of the carboxysome. This parameter was varied to optimize the fit of the model to observed photosynthetic rates, $CO_2$ efflux rates, and internal $C_i$ concentrations. The optimized model fit the data quite well and, in particular, captured the major regimes present in the data: a $C_i$-limited regime (less than 200 μM external $C_i$) where photosynthesis is increasing with $C_i$, $CO_2$ efflux is low, and the internal

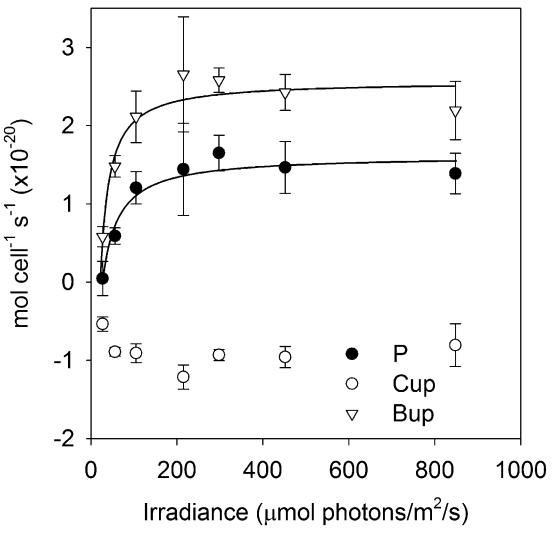


**Figure 4.** Rates of net photosynthesis (P), $CO_2$ uptake or efflux (Cup), and $HCO_3^-$ uptake (Bup) in *Prochlorococcus* spp. MED4 as a function of irradiance at saturating $C_i$ concentration (1,000 μM).

**Table II.** *Michaelis-Menten fits to photosynthesis and $C_i$ fluxes as a function of irradiance and SE values in the fitted parameters*

An offset, representing the irradiance at which rates are zero, was included in the fits. $I_k$, $I_B$, and the offsets are in $\mu$mol photons $m^{-2}$ $s^{-1}$, and $P_{max}$ and $B_{max}$ are in $\times 10^{-20}$ mol $cell^{-1}$ $s^{-1}$.

| Parameter | Fitted Value | SE |
|---|---|---|
| $I_k$ | 63 | 18 |
| $P_{max}$ | 1.62 | 0.22 |
| Photosynthetic rate offset | 27 | 5 |
| $I_B$ | 42 | 10 |
| $B_{max}$ | 2.57 | 0.17 |
| $HCO_3^-$ uptake offset | 22 | 5 |

$C_i$ pool is small; and a $C_i$-replete regime (greater than 200 $\mu$M external $C_i$) where photosynthesis is saturated for $C_i$ but the internal $C_i$ pool accumulates and $CO_2$ efflux becomes significant (Fig. 5). Two notable features of this best model are that the carboxysome $CO_2$ transfer coefficient is low ($2.4 \pm 0.5 \times 10^{-15}$ $cm^3$ $s^{-1}$) and there is excess Rubisco capacity (i.e. the $CO_2$-saturated Rubisco fixation rate per cell exceeds the observed maximal photosynthetic rate). To show that the best model predicts several features of the data better than other models, we ran two alternative models: the first with no excess Rubisco capacity (low Rubisco in Fig. 5) and the second with a 10-fold higher carboxysome $CO_2$ transfer coefficient ($10\times f_{c-x}$ in Fig. 5). Both of these alternative models do not fit the data as well, lacking the clear distinction between the two regimes evident in the best model. Instead, in these models, photosynthesis, $CO_2$ efflux, and the intracellular $C_i$ pool increase gradually until saturation around 1,000 $\mu$M external $C_i$ (Fig. 5, B and C).

The absolute values of the modeled intracellular $C_i$ are sensitive to internal pH and to the carboxysome $CO_2$ transfer coefficient. Because the only loss processes for $C_i$ inside the cell are photosynthesis and leakage of $CO_2$, the internal pool will build up until these loss rates match the $HCO_3^-$ uptake rate. Both these loss rates are dependent on the carboxysome $CO_2$ concentration, which in turn is dependent on pH and the carboxysome $CO_2$ transfer coefficient. The intracellular pH used in the model (7.35) was chosen from the range of reported values to obtain reasonable agreement between the modeled and observed absolute values of internal $C_i$. Nonetheless, agreement between the shape of the modeled intracellular $C_i$ curve and the data is meaningful and distinguishes the best model from alternative models (Fig. 5C).

A sensitivity analysis of the model was conducted, the details of which are presented in "Supplemental Data." Given the estimated parameter uncertainties for random error, the model is most sensitive to the internal pH and the turnover rate of Rubisco, although even the worst case scenarios for these parameters do not cause major issues with the model fit (Supplemental Text S1; Supplemental Tables S1–S3). There is also systematic uncertainty in the $K_m$ for Rubisco, which potentially ranges between 263 and 750 $\mu$M. First, we

**Table III.** *Model parameters*

| Symbol[a] | Definition | Value | Unit | Source |
|---|---|---|---|---|
| $c_x$ | $CO_2$ concentration | Varies | $\mu$M | |
| $b_x$ | $HCO_3^-$ concentration | Varies | $\mu$M | |
| $pH_e$ | Extracellular pH | 8 | – | Measurement |
| $pH_c$ | Cytoplasmic and carboxysomal pH | 7.35 | – | "Results" |
| $k_{cf}$ | $CO_2$ hydration rate constant in cytoplasm | $3 \times 10^{-2}$ | $s^{-1}$ | Uncatalyzed; Johnson (1982) |
| $k_{xf}$ | $CO_2$ hydration rate constant in carboxysome | 1,000 | $s^{-1}$ | Sufficient for equilibration |
| $m_R$ | Rubsico content | $6.6 \times 10^{-21}$ | mol active site $cell^{-1}$ | This study |
| $K_{m\text{-}R}$ | Rubisco one-half-saturation constant for $CO_2$ | 263 | $\mu$M | This study |
| $k_{cat\text{-}R}$ | Rubisco maximal turnover rate | 10.6 | $s^{-1}$ | Tcherkez et al. (2006) |
| $K_{m\text{-}B}$ | One-half-saturation constant for $HCO_3^-$ uptake | 82 | $\mu$M | This study |
| $V_{max\text{-}B}$ | Maximal $HCO_3^-$ uptake rate | $2.5 \times 10^{-20}$ | mol $cell^{-1}$ $s^{-1}$ | This study |
| $N_x$ | Number of carboxysomes per cell | 6 | | Ting et al. (2007) |
| $f_{c\text{-}c}$ | Cellular transfer coefficient for $CO_2$ | $1 \times 10^{-8}$ | $cm^3$ $s^{-1}$ | Assume diffusion limited (membrane is no barrier); Pasciak and Gavis (1974) |
| $f_{c\text{-}x}$ | Carboxysome transfer coefficient for $CO_2$ | $2 \times 10^{-15}$ | $cm^3$ $s^{-1}$ | Fitted to data |
| $f_{b\text{-}x}$ | Carboxysome transfer coefficient for $HCO_3^-$ | $6 \times 10^{-10}$ | $cm^3$ $s^{-1}$ | Assume diffusion limited (no barrier); Pasciak and Gavis (1974) |
| $V_c$ | Cytoplasmic volume | $1.8 \times 10^{-13}$ | $cm^3$ | Ting et al. (2007) |
| $V_x$ | Total carboxysome volume | $2.3 \times 10^{-15}$ | $cm^3$ | Ting et al. (2007) |

[a]Subscripts are as follows: b, bicarbonate; c, cytoplasm; e, external environment; f, forward rate constant; and x, carboxysome.

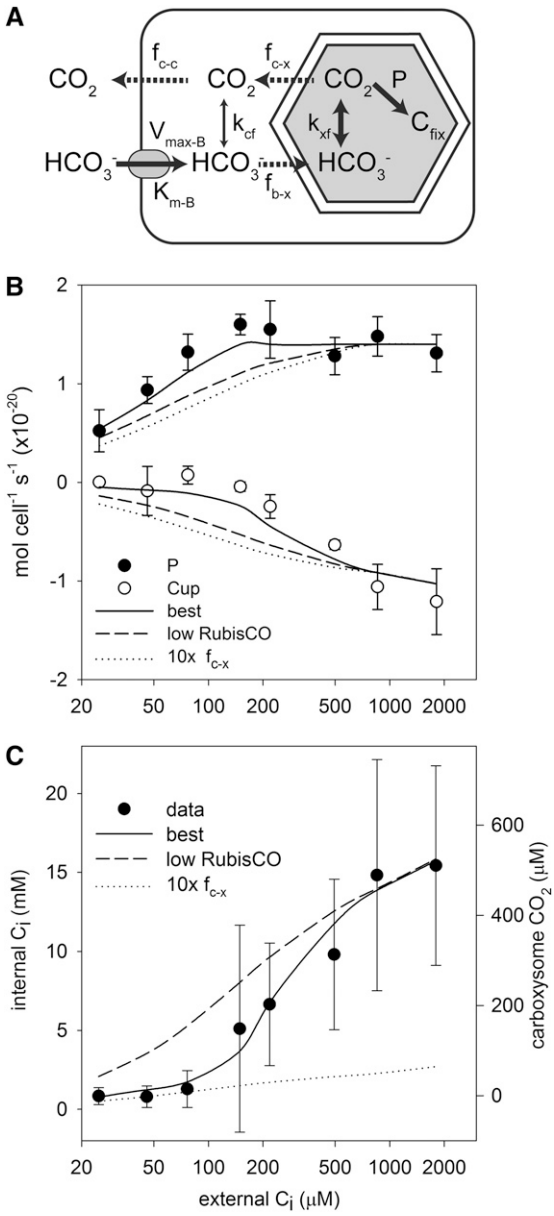


**Figure 5.** Model results. The model structure diagram (A) illustrates the active fluxes (solid arrows), passive fluxes (dashed arrows), and $CO_2$/$HCO_3^-$ interconversion (double-headed arrows) in the CCM, with the parameters controlling these fluxes indicated above each arrow (for notation, see Table III). Agreement of the various models with photosynthesis (P) and $CO_2$ flux (Cup) data (B) and the internal $C_i$ pool (C) is shown. Inferred carboxysome $CO_2$ concentrations were calculated as described in "Results."

considered increasing $K_m$ for Rubisco from our measured value of 263 to 520 $\mu$M, the value estimated for pH 7.35, assuming that the pH sensitivity is similar to that of Rubisco from *Anabaena variabilis* (Badger, 1980). This change does reduce model performance, primarily through increasing the internal $C_i$ pool at low external $C_i$, but the two regimes in the data are still resolved and the overall fit is reasonable (Supplemental Fig. S2). A further increase of $K_m$ for Rubisco to 750 $\mu$M, the value obtained by Scott et al. (2007), degrades the model fit further, with the most notable discrepancy being a higher modeled internal $C_i$ pool at low external $C_i$ (Supplemental Fig. S2). There is still some evidence for a distinction between the $C_i$-limited and $C_i$-replete regimes, but as $K_m$ for Rubisco increases, the model begins to look more similar to the low-Rubisco model, which lacks excess Rubisco capacity. The sensitivity of the model to $K_m$ for Rubisco is primarily a concern with respect to the effects of pH on $K_m$ for Rubisco. If confinement to the carboxysome imparts a lower apparent $K_m$ for Rubisco through environmental or allosteric effects, then the lower $K_m$ for Rubisco is more appropriate for our model, since such effects are not treated explicitly in the model.

### CCM Gene Expression

The expression of putative CCM genes and two housekeeping genes was measured in cultures acclimated to 150 and 1,000 $\mu$L L$^{-1}$ $CO_2$ (Fig. 6). None of the genes examined was significantly up- or down-regulated by the $CO_2$ treatments. The CCM genes assessed include components of the carboxysome shell (*csoS1*, *csoS2*, and *csoSCA*), the large and small subunits of Rubisco (*cbbL* and *cbbS*), a strong homolog to the low-affinity $Na^+$-dependent $HCO_3^-$ transporter A (*bicA2-1*), a weaker homolog to this transporter (*bicA2-2*), and a weak homolog to the high-affinity $Na^+$-dependent $HCO_3^-$ transporter A (*sbtA2*). The two housekeeping genes assessed, whose regulation was not expected to be affected by $CO_2$, were RNA polymerase $\sigma$ factor 70 (*rpoD*) and DNA gyrase subunit A (*gyrA*).

### *Prochlorococcus* spp. CCM Components in Marine Metagenomes

The Global Ocean Survey (GOS) metagenomes were searched for *Prochlorococcus* spp. CCM components using a reciprocal best BLAST hit approach. Carboxysome components were all present at reasonable abundances, although some components differed from the frequencies expected from the sequenced *Prochlorococcus* spp. genomes (Fig. 7). In particular, the abundances of CsoS4A, CsoS4B, and CbbS appear to be more than two times more common in the field than in the sequenced culture genomes. While we cannot rule out the possibility that their higher abundances are real, these genes are the smallest genes examined (CsoS4A, 261 nucleotides; CsoS4B, 246; and CbbS, 333), which leads us to suspect that the normalization procedures artificially increased abundance. A manual inspection of selected BLAST results for these genes confirmed that there was no difficulty in distinguishing *Prochlorococcus* spp. sequences from those of its closest relative, genus *Synechococcus* spp. We also searched for components of $CO_2$ uptake systems,

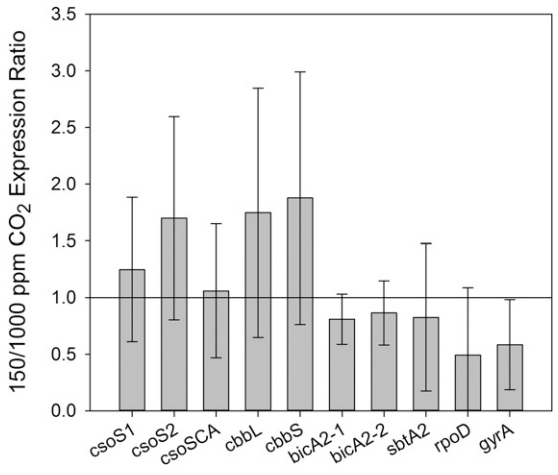


**Figure 6.** Effects of long-term acclimation to different $CO_2$ concentrations on the expression of genes involved in the CCM of *Prochlorococcus* spp. MED4 and selected housekeeping genes, as assessed using reverse transcription-qPCR. Although there is some indication that CCM genes are slightly up-regulated at low $CO_2$, none of the differences are statistically significant (Student's *t* test, $n = 3$). CCM genes include carboxysome shell proteins (*csoS1*, *csoS2*, and *csoSCA*), Rubisco (*cbbL* and *cbbS*), and potential $HCO_3^-$ transporters (*bicA2-1*, *bicA2-2*, and *sbtA2*). Housekeeping genes are $\sigma$ factor 70 (*rpoD*) and DNA gyrase (*gyrA*).

focusing on $CO_2$ hydration protein X (ChpX) and $CO_2$ hydration protein Y (ChpY) genes, since these genes are unique to cyanobacterial $CO_2$ uptake systems (Badger and Price, 2003; Ogawa and Mi, 2007). ChpX and ChpY sequences from marine and freshwater *Synechococcus* spp. were used to query the metagenomes in this case, since these genes are not present in sequenced *Prochlorococcus* spp. genomes. Only ChpX genes were found in the GOS metagenomes using a reciprocal best BLAST hit analysis. The mate pairs of these sequences were examined to see if any hit to *Prochlorococcus* spp. Out of 134 ChpX sequences found, 127 mate pairs had best hits to genes in *Synechococcus* spp. genomes and three hit to components of a heme uptake system in *Prochlorococcus* spp. MIT9202, with the remaining mate pairs (four) hitting heterotrophic bacteria.

## DISCUSSION

### The CCM of *Prochlorococcus* spp. Is Functional and Efficient

The $K_P$ was approximately 30 $\mu$M, much lower than the approximately 2 mM $C_i$ available in seawater, showing that photosynthesis is fully saturated with $C_i$ in the ocean. This low $K_P$ is similar to that of cyanobacteria with a greater repertoire of $HCO_3^-$ and $CO_2$ uptake systems (Badger and Andrews, 1982; Price et al., 2004; Rae et al., 2011). As discussed in more detail below, neither $K_P$ nor any other parameter was affected by growth at either 150 or 1,000 $\mu$L $L^{-1}$ $CO_2$, so the two treatments will not be distinguished here. $HCO_3^-$ uptake as a function of $C_i$ availability followed Michaelis-Menten kinetics, consistent with a single transporter dominating $HCO_3^-$ uptake. The $K_B$ was between 80 and 130 $\mu$M, similar to $K_B$ values for BicA transporters from several different cyanobacteria (38–171 $\mu$M) and, most notably, close to the $K_B$ for BicA from the marine *Synechococcus* sp. WH8102 (approximately 75 $\mu$M; Price et al., 2004), suggesting that the BicA homolog in *Prochlorococcus* spp. is the primary $HCO_3^-$ transporter. The homolog of the high-affinity SbtA may be active in *Prochlorococcus* spp., but it would likely only be responsible for a small fraction of overall $HCO_3^-$ uptake under the conditions examined, since the $K_B$ of SbtA is much lower (2–16 $\mu$M; Shibata et al., 2002; Price et al., 2004). $HCO_3^-$ uptake continues to increase after photosynthesis is saturated for $C_i$, and this additional $HCO_3^-$ uptake simply leaks back out of the cell as $CO_2$. However, it does increase the internal $C_i$ pool, and thus the $CO_2$ concentration in the carboxysome, which could serve to reduce photorespiration by increasing the $CO_2$-to-oxygen ratio.

Net $CO_2$ efflux was observed from the cells at $C_i$ concentrations of 200 $\mu$M and above (Fig. 1). As shown by the addition of $^{13}C^{18}O$-labeled $C_i$, the $CO_2$ originates

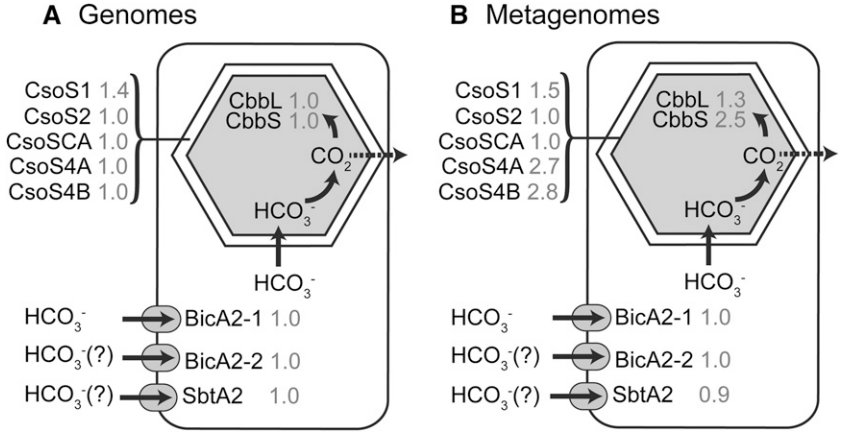


**Figure 7.** Frequency of *Prochlorococcus* spp. CCM components in genomes (A) and GOS metagenomes (B). *Prochlorococcus* spp. CCM components in the genomes were identified by BLAST analysis. In the metagenomes, *Prochlorococcus* spp. CCM components were identified by reciprocal BLAST analysis, and the counts were length normalized relative to RecA and then divided by the mean counts of four single-copy genes to estimate CCM genes per *Prochlorococcus* spp. genome (gray numbers next to protein names).

from freshly transported $C_i$ rather than from respiration, which would produce predominantly $^{12}CO_2$. The effluxed $CO_2$ is entirely depleted of $^{18}O$ label, indicating that the $C_i$ has undergone many hydration/dehydration cycles prior to exiting the cell (Tchernov et al., 1997). Since the only known CA in *Prochlorococcus* spp. is in the carboxysome (So et al., 2004), this shows that the leaked $CO_2$ originates in the carboxysome, where CA removes the $^{18}O$ label and increases the $CO_2$ concentration, driving efflux. Unlike many cyanobacteria that have active $CO_2$-to-$HCO_3^-$ conversion mechanisms to take up and recover leaked $CO_2$, *Prochlorococcus* spp. has no known $CO_2$ recovery mechanisms. The observation of $CO_2$ efflux from the cell is consistent with this, as is the pattern of $^{18}O$ exchange in the light. Upon illumination, cyanobacteria that possess $CO_2$ recovery mechanisms draw down $^{13}C^{18}O^{18}O$ and $^{13}C^{18}O^{16}O$ while $^{13}C^{16}O^{16}O$ increases, whereas cyanobacteria with inactivated $CO_2$ recovery systems only show increases of $^{13}C^{16}O^{16}O$, as was observed here for *Prochlorococcus* spp. (Maeda et al., 2002; Whitehead et al., 2014).

If there are no $CO_2$ recovery mechanisms, $HCO_3^-$ uptake into the cytoplasm is the only active transport step, and the efficiency of the CCM can be estimated as the rate of $HCO_3^-$ uptake divided by the photosynthetic rate (Tchernov et al., 1997; Hopkinson et al., 2011). Under growth conditions, which are similar to typical conditions in the ocean, the CCM is remarkably efficient, with only two molecules of $HCO_3^-$ transported per $CO_2$ molecule fixed. For comparison, the diatom *Phaeodactylum tricornutum* transports 3.5 molecules of $HCO_3^-$ per $CO_2$ fixed (Hopkinson et al., 2011) and *Synechococcus* sp. WH7803 transports six molecules of $HCO_3^-$ per $CO_2$ fixed (Tchernov et al., 1997), making the *Prochlorococcus* spp. CCM the most efficient of the few that have been examined.

### The Minimal CCM Model Is Consistent with Physiological Data

The simple CCM indicated by an analysis of *Prochlorococcus* spp. genomes implies that there should be straightforward relationships between the intracellular $C_i$ pool, photosynthesis, and $CO_2$ efflux. Without a $CO_2$ recovery mechanism, $CO_2$ efflux should be linearly related to the $CO_2$ gradient between the carboxysome and the extracellular solution. Because the $CO_2$ concentration in the carboxysome was always much greater than the $CO_2$ in the external solution (maximum of 15 $\mu$M), to first order $CO_2$ efflux should be directly related to the $CO_2$ concentration in the carboxysome, which is proportional to the intracellular $C_i$ pool. A linear relationship was observed between the $CO_2$ efflux rate and the intracellular $C_i$ pool, consistent with the simple CCM model (Fig. 3B). However, a closer examination of the data shows that there are two distinct regimes to the data. In the first regime (less than 200 $\mu$M external $C_i$), photosynthesis increases with external $C_i$ while little to no $CO_2$ efflux is observed and the intracellular $C_i$ pool remains small (Figs. 1 and 3). In the second regime, at higher external $C_i$ (greater than 200 $\mu$M), photosynthesis is saturated for $C_i$ but the internal $C_i$ pool continues to increase and $CO_2$ efflux becomes significant.

The CCM model is able to explain these two regimes and shows that the key characteristics producing these two regimes are excess Rubisco capacity and a low permeability of the carboxysome to $CO_2$, as illustrated by the failure of alternative models lacking these characteristics to match the data (Fig. 5). In many algae, there is little excess Rubisco capacity, so photosynthesis should follow a Michaelis-Menten relationship with the $CO_2$ concentration around Rubisco (Badger et al., 1980; Losh et al., 2013; Hopkinson, 2014). In *Prochlorococcus* spp., $CO_2$ efflux should be linearly related to the $CO_2$ concentration in the carboxysome and so would also show a Michaelis-Menten relationship if there was no excess Rubisco capacity. This is clearly not the case here: photosynthesis became saturated at an intracellular $C_i$ concentration of approximately 5 mM when $CO_2$ in the carboxysome was approximately 200 $\mu$M, and only minimal $CO_2$ efflux was observed (Fig. 3C). Further increase in the carboxysome $CO_2$ concentration (to 500 $\mu$M at 2 mM external $C_i$) did not lead to higher rates of photosynthesis, meaning that a factor other than $CO_2$, such as electron transport or ribulose 1,5-bisphosphate (RuBP) regeneration, was limiting carbon fixation in this regime.

Consistent with this, an estimate of the maximal $CO_2$ fixation rate by Rubisco at saturating $CO_2$ based on quantitative measurements of Rubisco abundance combined with estimated turnover rates (10.6 $s^{-1}$ active $site^{-1}$ and eight active sites per molecule) shows that there was approximately 4-fold excess Rubisco capacity above the measured rates of $CO_2$ fixation. This excess Rubisco capacity contributes to the low $K_P$ of *Prochlorococcus* spp. and may explain how the low $K_P$ is achieved in the absence of $CO_2$ recovery mechanisms or high-affinity $HCO_3^-$ transporters. Other cyanobacteria with a greater repertoire of $C_i$ transporters have little excess Rubisco capacity (Whitehead et al., 2014). Once photosynthesis is saturated for $CO_2$, further $HCO_3^-$ import leads to the buildup of the intracellular $C_i$ pool and carboxysome $CO_2$ concentration, such that the rate of $CO_2$ leakage matches the rate of $HCO_3^-$ import in excess of photosynthesis.

Given the reduced features of the *Prochlorococcus* spp. CCM, the carboxysome must be a significant barrier to $CO_2$ efflux. The best model fit was obtained with a carboxysome $CO_2$ transfer coefficient of $2.4 \times 10^{-15}$ $cm^3$ $s^{-1}$ or, approximating the carboxysomes as spheres of 45-nm radius (Ting et al., 2007), a permeability of $1 \times 10^{-5}$ cm $s^{-1}$. The mass transfer coefficient is approximately 4 orders of magnitude lower than the diffusion-controlled transfer coefficient ($9 \times 10^{-10}$ $cm^3$ $s^{-1}$), obtained assuming that the carboxysome structure does not hinder $CO_2$ diffusion (Pasciak and Gavis, 1974). A maximal estimate of the carboxysome $CO_2$ transfer

coefficient can be made using our measurements of Rubisco content and one-half-saturation constant for $CO_2$ combined with literature values for the maximum turnover rate of cyanobacterial Rubisco (Table III) to calculate the minimal $CO_2$ concentration in the carboxysome (84 $\mu$M) required to match the maximal rate of photosynthesis. Since membranes are highly permeable to $CO_2$, the resistance of the carboxysome should be the major control on $CO_2$ efflux, in which case the efflux rate can be described by the $CO_2$ transfer coefficient for the carboxysome ($f_{c\text{-}x}$) and the $CO_2$ concentration difference between the carboxysome and the extracellular solution: efflux = $f_{c\text{-}x}N_x([CO_2]_x - [CO_2]_e)$, where $N_x$ = the number of carboxysomes per cell. Using the minimal carboxysome $CO_2$ concentration and the observed efflux rates, the maximal carboxysome $CO_2$ transfer coefficient was estimated as $2.4 \times 10^{-14}$ cm$^3$ s$^{-1}$, or permeability of $1 \times 10^{-4}$ cm s$^{-1}$, still several orders of magnitude lower than the diffusion-controlled estimate. These best and maximal permeability values are very similar to values that have been found necessary to obtain efficient CCMs in previous models ($1 \times 10^{-5}$ to $2.5 \times 10^{-4}$ cm s$^{-1}$; Reinhold et al., 1987, 1991). If the carboxysome did not act as a $CO_2$ barrier, the efficiency of the CCM would be massively reduced, limiting its usefulness. The carboxysome has long been postulated to be a barrier to $CO_2$ efflux (Reinhold et al., 1987), and analysis of isolated carboxysomes lacking CA has provided support for this hypothesis (Dou et al., 2008), but the simple structure of the *Prochlorococcus* spp. CCM has allowed us to quantitatively assess the extent to which the carboxysome prevents $CO_2$ efflux.

### Regulation of the CCM by $CO_2$

In most microalgae, $CO_2$ availability is the primary factor regulating CCM expression, with decreased $CO_2$ availability inducing up-regulation of the CCM (Woodger et al., 2005; Matsuda et al., 2011). One common manifestation of CCM up-regulation is a decline in $K_P$ and $K_B$ (Kaplan et al., 1980; Rost et al., 2003). Despite some reduction in $K_P$ and $K_B$ at 150 $\mu$L L$^{-1}$ $CO_2$, these parameters were not significantly different from their values at 1,000 $\mu$L L$^{-1}$ $CO_2$, nor were any other physiological characteristics ($P_{max}$, $B_{max}$, and $CO_2$ efflux; Table I). At the genetic level, no CCM genes were differentially expressed between the two long-term $CO_2$ acclimation treatments (Fig. 6). Consistent with this lack of a long-term response to $CO_2$ treatment is the absence of canonical CCM transcription factors (CcmR and CmpR) in the *Prochlorococcus* spp. genome (Omata et al., 2001; Woodger et al., 2007; Nishimura et al., 2008). However, *Prochlorococcus* spp. does have a $P_{II}$ protein, which contributes to CCM regulation in some cyanobacteria (Palinska et al., 2002), and we did not explore the potential for short-term responses to $CO_2$ deficiency, which could induce transient changes in gene and protein expression as observed in response to nitrogen starvation in *Prochlorococcus* spp. (Tolonen et al., 2006). Another $\alpha$-cyanobacterium, *Synechococcus* sp. WH5701, also showed no physiological changes when acclimated to different $CO_2$ concentrations, but some changes in gene expression were observed (Rae et al., 2011). This is not the case for all $\alpha$-cyanobacteria, as some have strong physiological responses to changes in long-term $CO_2$ availability (Hassidim et al., 1997; Whitehead et al., 2014).

Some algae are able to take advantage of rising ocean $CO_2$ concentrations by down-regulating their CCMs and redirecting energy toward increased growth (Rost et al., 2008; Hopkinson et al., 2011). The lack of response to $CO_2$ suggests that *Prochlorococcus* spp. cannot take advantage of rising ocean $CO_2$ concentrations in this way. Consistent with this, the growth of *Prochlorococcus* spp. does not increase with increasing $CO_2$ (Fu et al., 2007). Although, in principle, the increased extracellular $CO_2$ concentration should decrease $CO_2$ leakage, conserving some energy, the $CO_2$ concentration in the carboxysome is so high (approximately 500 $\mu$M) compared with external $CO_2$ (5 $\mu$M at 150 $\mu$L L$^{-1}$ $CO_2$ and 32 $\mu$M at 1,000 $\mu$L L$^{-1}$ $CO_2$) that the change in the absolute gradient, which controls the leakage rate, would be small.

### *Prochlorococcus* spp. CCM Genes in the Environment

The set of CCM genes found in *Prochlorococcus* spp. genomes obtained from cultured isolates is nearly constant, with the exception of some small variations in the carboxysome proteins (Badger et al., 2006; Roberts et al., 2012). The genetic complement and physiological characteristics of isolated *Prochlorococcus* spp. strains are generally similar to those in the environment, but some differences have been identified (Martiny et al., 2009; Rusch et al., 2010). To determine if the complement of CCM genes found in natural *Prochlorococcus* spp. populations is similar to that of cultured isolates, we searched the GOS metagenomes for core CCM genes using a reciprocal BLAST approach to ensure that only *Prochlorococcus* spp. sequences were matched. The natural populations show a similar gene frequency to cultured isolates, suggesting that the CCM in the environment is similar to that in cultured strains (Fig. 7). The inferred high abundance of short carboxysome genes (CsoS4A, CsoS4B, and CbbS) is thought to be an artifact due to the short length of these genes. We also searched the metagenomes for genes diagnostic for $CO_2$ uptake systems in cyanobacteria (ChpX and ChpY; Shibata et al., 2001; Maeda et al., 2002). Using mate-pair analysis, three sequences were identified that may have been in *Prochlorococcus* spp., but in all three cases, the mate pairs hit components of a heme uptake system, which itself is thought to be horizontally acquired and rare in *Prochlorococcus* spp. (Hopkinson and Barbeau, 2012). These results suggest that environmental *Prochlorococcus* spp., like their cultured representatives, generally cannot take up $CO_2$, although on extremely rare occasions they may have this ability.

## CONCLUSION

The agreement between the CCM model and physiological data suggests we have a good understanding of the mechanics of the *Prochlorococcus* spp. CCM and, to the extent that it is similar to the CCMs in other cyanobacteria, a good understanding of those CCMs as well. However, some questions about the function and ecological role of the *Prochlorococcus* spp. CCM remain. The CCM is quite efficient, pumping two molecules of $HCO_3^-$ per $CO_2$ fixed, compared with a few other marine algae that have been studied. This may help *Prochlorococcus* spp. conserve energy and outcompete other algae, especially deep in the ocean where light intensity is low, but the efficiency of the CCM has only been assessed in a few selected algae. Although this efficiency is impressive, *Prochlorococcus* spp. shows the potential to be even more efficient. Photosynthesis becomes saturated at low $C_i$ concentrations (approximately 200 $\mu$M), when essentially no $CO_2$ efflux is observed, and the CCM is perfectly efficient in that every $HCO_3^-$ molecule imported is fixed. However, as $C_i$ increases further, the cell imports more $HCO_3^-$, which is not fixed but instead leaks back out of the cell. The increased rates of $HCO_3^-$ uptake do increase the intracellular $C_i$ pool and carboxysomal $CO_2$ concentration, which would help to reduce photorespiration by further increasing the $CO_2$-to-oxygen ratio. Nonetheless, the *Prochlorococcus* spp. CCM is surprisingly effective and efficient despite its simplicity, another example of the remarkable adaptations that allow this simple organism to dominate large parts of the ocean. More generally, this study confirms that the CCMs of $\alpha$-cyanobacteria, even with the minimal components present in *Prochlorococcus* spp., function similarly to the well-studied CCMs of $\beta$-cyanobacteria (Whitehead et al., 2014).

## MATERIALS AND METHODS

### Culturing

*Prochlorococcus* spp. MED4 (CCMP 1986) was obtained from the National Center for Marine Algae and Microbiota and maintained in PRO99 medium using natural Gulf Stream seawater as a base (Moore et al., 2007). The seawater base was sterilized by autoclaving, and the nutrient stocks were 0.2 $\mu$m filtered. All culture vessels were acid washed (10% [v/v] HCl) and thoroughly rinsed with deionized water and then ultrapure (greater than 18 M$\Omega$ cm$^{-1}$) water. Cultures were maintained at 18°C and a light intensity of 100 $\mu$mol photons m$^{-2}$ s$^{-1}$ on a light/dark cycle of 16/8 h. Growth was tracked by measurement of in vivo chlorophyll fluorescence. Culture $CO_2$ conditions were controlled by bubbling with premixed $CO_2$-air mixtures (150 or 1,000 $\mu$L L$^{-1}$ $CO_2$). To ensure that the bubbling rate was sufficient to achieve equilibrium, medium pH was routinely measured using Thymol Blue (Zhang and Byrne, 1996), and dissolved $C_i$ was measured on occasion using membrane inlet mass spectrometry (MIMS). Cultures were allowed to acclimate for at least 2 weeks to the $CO_2$ conditions. Cultures were always harvested in midmorning, approximately 4 h after the light period began, to ensure that cells were in a consistent state with respect to diel variability.

### Cell Counts

Samples from experimental suspensions were preserved with glutaraldehyde (0.125% [v/v] final concentration), frozen, and stored in liquid nitrogen. Just prior to analysis, samples were defrosted at 35°C and diluted 400-fold in 0.2 $\mu$m filtered artificial seawater. Cells were counted flow cytometrically as described previously (Worden and Binder, 2003).

### $C_i$ Acquisition

A membrane inlet mass spectrometer (Pfeiffer QMS220) was used to measure net $CO_2$ and $HCO_3^-$ fluxes and photosynthetic oxygen production. Cells were harvested by centrifugation at 11,000*g* for 15 min, resuspended in 1 to 2 mL of $C_i$-free artificial seawater, centrifuged again at 7,000*g* for 3 min, and finally resuspended in 1 mL of $C_i$-free artificial seawater with 20 mM Tris buffer at pH 8 for experimentation. This cell suspension was then placed in the cuvette of the MIMS system. Fifty micromolar acetazolamide, a CA inhibitor that does not pass through cell membranes, was added to ensure that $CO_2$ hydration and $HCO_3^-$ dehydration rates were at background, uncatalyzed rates. To assess $C_i$ acquisition as a function of $C_i$ availability, any residual $C_i$ in the assay solution was first consumed through photosynthesis by turning on a light-emitting diode light (200 $\mu$mol photons m$^{-2}$ s$^{-1}$). $^{13}$C-labeled $C_i$ was then gradually added back to the sample using alternating dark and light phases to determine net $CO_2$ and $HCO_3^-$ fluxes into or out of the cells and net photosynthesis rates following the methods of Badger et al. (1994). Net photosynthetic rates were determined from the rate of oxygen production. Net $CO_2$ flux was calculated from the extent to which the $CO_2$ concentration was drawn down below (uptake) or raised above (efflux) equilibrium. Net $HCO_3^-$ uptake was then calculated as the difference between photosynthesis and net $CO_2$ flux (with positive $CO_2$ flux indicating uptake and negative indicating efflux). Rates were normalized by cell number as counted using flow cytometry. Michaelis-Menten curves were fit to the net photosynthesis and $HCO_3^-$ uptake data.

After each dark cycle, $CO_2$ concentrations rose above equilibrium levels, which we interpret to be the result of leakage of accumulated intracellular $C_i$ out of the cell. The rate of leakage can be determined by tracking the $CO_2$ concentration and accounting for net loss due to hydration (Supplemental Fig. S3):

$$Efflux = \frac{d[CO_2]}{dt} + k_f\left([CO_2] - [CO_2]_{eq}\right) \quad (1)$$

where $k_f$ is the spontaneous $CO_2$ hydration rate, $[CO_2]_{eq}$ is the $CO_2$ concentration at equilibrium, $d$ indicates differentiation, and $t$ is time. The leakage rate can then be integrated over time until the $CO_2$ concentration returns to equilibrium, giving the total amount of $C_i$ that was lost from the cell, which is used here as a measure of the intracellular $C_i$ pool (Supplemental Fig S3). This assumes that the main loss process for accumulated $C_i$ is by leakage of $CO_2$ out of the cell. The approach is similar to that taken by Badger et al. (1985), except that in their experiments, CA was added, so that the $CO_2$ measurements were a direct measurement of the total external $C_i$ concentration. Recent comparisons of the MIMS method with the more traditional silicone oil centrifugation method found that the approaches were generally similar, but the MIMS method underestimated $C_i$ pools at low external $C_i$ in some cases (Whitehead et al., 2014). The cytoplasmic volume, which is required to calculate the internal $C_i$ concentration, was estimated from the three-dimensional reconstructions of *Prochlorococcus* spp. MED4 cells of Ting et al. (2007). The total cell volume was calculated assuming that the cell is a sphere of diameter 0.7 $\mu$m, and then the thylakoid volume, estimated to take up approximately 30% of the cell volume by analysis of the images in Ting et al. (2007), was subtracted from the total volume to calculate the cytoplasmic volume.

In another set of experiments, the effect of light intensity on $C_i$ uptake was assessed similarly, except that 1 mM $C_i$ was added and light intensity was gradually increased from 25 to 850 $\mu$mol photons m$^{-2}$ s$^{-1}$.

### Rubisco Quantification and Kinetics

Quantification of Rubisco protein was performed as described by Losh et al. (2013). Briefly, cells were pelleted via centrifugation, and total protein was extracted by vortexing and boiling the pellet for 5 min in SDS buffer (50 mM Tris-HCl, 2% [w/v] SDS, 10% [v/v] glycerol, and 12.5 mM EDTA). Total protein was quantified using the bicinchoninic acid assay against a bovine serum albumin protein standard according to the manufacturer's instructions (Pierce, Thermo Scientific). Picomoles of CbbL (the large subunit of Rubisco) were determined through quantitative western blotting with global antibodies and standards according to the manufacturer's instructions (Agrisera). Since there are equimolar concentrations of CbbL and CbbS (the small subunit), total

Rubisco protein was calculated from the pmol of CbbL and masses of 52.57 and 12.94 kD for CbbL and CbbS, respectively (Rocap et al., 2003).

The one-half-saturation constant for Rubisco $CO_2$ fixation was determined at 20°C in crude protein extracts using a $^{14}C$ assay. In 2 mL of $N_2$-sparged gas-tight vials, 10 $\mu$g of Rubisco (in 20 $\mu$L of crude extract) was added to 500 $\mu$L of assay buffer (50 mM Bicine, 20 mM, $MgCl_2$, 1 mM EDTA, 5 mM dithiothreitol, 0.1 mg $mL^{-1}$ CA, and 0.4 mM RuBP, pH 8, bubbled with $N_2$ to remove all $CO_2$ and oxygen). The reaction was started by the addition of varying amounts of $NaH^{14}CO_3$ from 0 to 1 M, and vials were incubated for 4 min. Reaction was stopped by the addition of 0.5 mL of 6 N HCl. Vials were left to degas of inorganic $^{14}C$ overnight. Organic $^{14}C$ was counted with a scintillation counter (PerkinElmer). To confirm that there was no nonspecific activity, we tested $^{14}C$ assays with activated crude extract without RuBP and used these values as blanks

## Gene Expression

The relative expression of putative CCM genes at 150 and 1,000 $\mu$L $L^{-1}$ $CO_2$ was assessed using reverse transcription-quantitative polymerase chain reaction (qPCR). *Prochlorococcus* spp. cultures were allowed to acclimate to 150 and 1,000 $\mu$L $L^{-1}$ $CO_2$ as described above, at which point cells were harvested by centrifugation and RNA was isolated using TRIzol (Invitrogen) following the manufacturer's instructions. The isolated total RNA was treated with 2 units of amplification-grade DNase to remove any potential contaminating DNA. One microgram of total RNA was reverse transcribed using random hexamer primers to complementary DNA (cDNA) with SuperScript III reverse transcriptase (Invitrogen). Parallel reactions were run without reverse transcriptase for use as no-template controls in the qPCR analysis.

Relative abundances of putative CCM genes were quantified by qPCR using a Bio-Rad iCycler iQ. Primers for the CCM genes and controls were designed using the *Prochlorococcus* spp. MED4 genome sequence and are listed in Supplemental Table S4. qPCR mixtures (25 $\mu$L) consisted of 12.5 $\mu$L of Bio-Rad iQ SYBR Green 2× Supermix, 0.75 $\mu$L of forward and reverse primers (200 nM final concentration), 9 $\mu$L of ultrapure water, and 2 $\mu$L of cDNA or no-template control. Temperature profiles for the PCR consisted of an initial 10 min at 50°C and then 5 min at 95°C, followed by 45 cycles of 95°C for 10 s (melting) and 30 s at 58°C (annealing and extension), and finally 1 min at 95°C and 1 min at 55°C. Five dilutions of genomic DNA were analyzed for each gene to produce a standard curve for the quantification of relative gene expression based on the cycle at which fluorescence crossed a threshold level. Following each qPCR, a melting-curve analysis was performed, and selected products were run on a 1% (w/v) agarose gel to verify that a single product of the expected length was amplified. No-template controls amplified much later in the reaction than cDNA samples (worst case three cycles later).

## Metagenomic Analyses

Putative CCM genes from the 18 publicly available *Prochlorococcus* spp. genomes were used to search for homologs in the GOS metagenomic data set using a reciprocal BLAST analysis. These genes include components of the carboxysome shell (CsoS1, CsoS2, CsoSCA, CsoS4A, and CsoS4B; National Center for Biotechnology Information accession numbers WP011819929, WP011132186, WP011132187, WP011132188, and WP011132189), Rubisco large and small subunits (CbbL and CbbS; WP011130576 and WP011132185), and putative bicarbonate transporters (BicA2-1, BicA2-2, and SbtA2; WP011131853, WP011132278, and WP011131852). Sets of protein sequences from the *Prochlorococcus* spp. genomes were compiled and used as query sequences in a tBLASTn search against the GOS metagenomes, keeping hits with E-values less than 1E-5. These metagenome sequences were then used as query sequences in a BLASTx search against a database of 206 marine bacterial genomes (Hopkinson and Barbeau, 2012). If the top BLASTx hit in this search was a *Prochlorococcus* spp. sequence used in the initial tBLASTn search (i.e. a reciprocal best BLAST hit), then the metagenome sequence was retained as a member of the protein family of interest. The raw sequence counts were scaled by the average length of genes in the family of interest relative to the length of recombinase A (RecA; i.e. length-corrected counts = raw counts × [RecA length/gene of interest length]) to correct for more frequent sampling of longer genes. CCM gene frequency, in genes per *Prochlorococcus* spp. genome, was calculated by dividing the length-corrected counts by the average number of single-copy *Prochlorococcus* spp. genes found (DNA gyrase B, HSP70, RecA, and RNA polymerase B). Because the number of counts at most individual GOS sites was low, counts were summed over the entire GOS data set prior to normalization by single-copy gene number.

## Modeling

A numerical model of the *Prochlorococcus* spp. CCM, similar in structure to that of Reinhold et al. (1987), was used to assess the consistency of the data with the streamlined CCM indicated by genomic analysis (Fig. 5A). $CO_2$ and $HCO_3^-$ concentrations are modeled in the cytoplasm and carboxysome, with $CO_3^{2-}$ treated implicitly as part of the $HCO_3^-$ pool, since equilibrium between these species is established very rapidly (Zeebe and Wolf-Gladrow, 2001). The only active transport is the import of $HCO_3^-$ into the cytoplasm, which is described by Michaelis-Menten kinetics and parameterized from the $HCO_3^-$ uptake data. $HCO_3^-$ accumulates in the cytoplasm, which lacks CA, and then diffuses into the carboxysome, which is taken to be highly permeable to $HCO_3^-$ as a result of positively charged pores in the carboxysome shell (Klein et al., 2009; Kinney et al., 2011). In the carboxysome, CA catalyzes the conversion of $HCO_3^-$ to $CO_2$, elevating the $CO_2$ concentration around Rubisco. Rubisco fixes $CO_2$ in the carboxysome at a rate dependent on the $CO_2$ concentration and capped at the observed maximal $CO_2$ fixation rate to simulate limitation by another factor such as electron transport rate or RuBP regeneration. $CO_2$ can diffuse passively out of the carboxysome and cell, as parameterized by transfer coefficients. The transfer coefficient between the cytoplasm and bulk solution was calculated assuming that the cytoplasmic membrane is not a significant barrier to $CO_2$ flux, as has been found for many other algae and red blood cells (Silverman et al., 1981; Hopkinson et al., 2011). The $CO_2$ transfer coefficient for carboxysomes has not been determined and instead was optimized to fit the observed rates of photosynthesis, $CO_2$ efflux, and the internal $C_i$ concentration. The model is described by a system of differential equations:

$$\frac{dc_c}{dt} = -k_{cf}c_c + k_{cr}b_c + \frac{1}{V_c}\left[f_{c-c}(c_e - c_c) + f_{c-x}(c_x - c_c)\right] \quad (2)$$

$$\frac{db_c}{dt} = k_{cf}c_c - k_{cr}b_c + \frac{1}{V_c}\left[f_{b-x}(b_x - b_c) + B_{up}\right] \quad (3)$$

$$\frac{dc_x}{dt} = -k_{xf}c_x + k_{xr}b_x + \frac{1}{V_x}\left[f_{c-x}N_x(c_c - c_x) - P\right] \quad (4)$$

$$\frac{db_x}{dt} = k_{xf}c_x - k_{xr}b_x + \frac{1}{V_x}\left[f_{b-x}N_x(b_c - b_x)\right] \quad (5)$$

where the $HCO_3^-$ uptake ($B_{up}$) and photosynthetic ($P$) rates are described as follows:

$$B_{up} = \frac{V_{max-B}b_e}{K_{m-B} + b_e} \quad (6)$$

$$P = min\left(\frac{k_{cat-R}m_R c_x}{K_{m-R} + c_x}, P_{max}\right) \quad (7)$$

The notation is detailed in Table III.

Sequence data from this article can be found in the GenBank/EMBL data libraries under accession numbers WP011819929, WP011132186, WP011132187, WP011132188, WP011132189, WP011130576, WP011132185, WP011131853, WP011132278, and WP011131852.

## Supplemental Data

The following materials are available in the online version of this article.

**Supplemental Figure S1.** Rubisco fixation rate as a function of $CO_2$.

**Supplemental Figure S2.** Effect of Rubisco $K_m$ on model-data agreement.

**Supplemental Figure S3.** Determination of the internal $C_i$ pool from $CO_2$ efflux.

**Supplemental Table S1.** Model parameters and variability.

**Supplemental Table S2.** Results of sensitivity analysis.

**Supplemental Table S3.** Interactions between model parameters.

**Supplemental Table S4.** qPCR primers.

**Supplemental Text S1.** Model sensitivity analysis.

## ACKNOWLEDGMENTS

We thank François Morel (Princeton University) for helpful advice and discussions, and two anonymous reviewers for careful analysis of the work and helpful comments that improved the article.

Received July 25, 2014; accepted October 10, 2014; published October 14, 2014.

## LITERATURE CITED

**Badger MR** (1980) Kinetic properties of ribulose 1,5-bisphosphate carboxylase/oxygenase from *Anabaena variabilis*. Arch Biochem Biophys **201:** 247–254

**Badger MR, Andrews TJ** (1982) Photosynthesis and inorganic carbon usage by the marine cyanobacterium, *Synechococcus* sp. Plant Physiol **70:** 517–523

**Badger MR, Bassett M, Comins HN** (1985) A model for $HCO_3^-$ accumulation and photosynthesis in the cyanobacterium *Synechococcus* sp.: theoretical predictions and experimental observations. Plant Physiol **77:** 465–471

**Badger MR, Hanson D, Price GD** (2002) Evolution and diversity of $CO_2$ concentrating mechanisms in cyanobacteria. Funct Plant Biol **29:** 161–173

**Badger MR, Kaplan A, Berry JA** (1980) Internal inorganic carbon pool of *Chlamydomonas reinhardtii*: evidence for a carbon dioxide concentrating mechanism. Plant Physiol **66:** 407–413

**Badger MR, Palmqvist K, Yu J** (1994) Measurement of $CO_2$ and $HCO_3^-$ fluxes in cyanobacteria and microalgae during steady-state photosynthesis. Physiol Plant **90:** 529–536

**Badger MR, Price GD** (2003) $CO_2$ concentrating mechanisms in cyanobacteria: molecular components, their diversity and evolution. J Exp Bot **54:** 609–622

**Badger MR, Price GD, Long BM, Woodger FJ** (2006) The environmental plasticity and ecological genomics of the cyanobacterial $CO_2$ concentrating mechanism. J Exp Bot **57:** 249–265

**Belkin S, Mehlhorn RJ, Packer L** (1987) Proton gradients in intact cyanobacteria. Plant Physiol **84:** 25–30

**Bertilsson S, Berglund O, Karl DM, Chisholm SW** (2003) Elemental composition of marine *Prochlorococcus* and *Synechococcus*: implications for the ecological stoichiometry of the sea. Limnol Oceanogr **48:** 1721–1731

**Dou Z, Heinhorst S, Williams EB, Murin CD, Shively JM, Cannon GC** (2008) $CO_2$ fixation kinetics of *Halothiobacillus neapolitanus* mutant carboxysomes lacking carbonic anhydrase suggest the shell acts as a diffusional barrier for $CO_2$. J Biol Chem **283:** 10377–10384

**Falkner G, Horner F, Werdan K, Heldt HW** (1976) pH changes in cytoplasm of the blue-green alga *Anacystis nidulans* caused by light-dependent proton flux into the thylakoid space. Plant Physiol **58:** 717–718

**Fu FX, Warner ME, Zhang YH, Feng YY, Hutchins DA** (2007) Effects of increased temperature and $CO_2$ on photosynthesis, growth, and elemental ratios in marine *Synechococcus* and *Prochlorococcus* (cyanobacteria). J Phycol **43:** 485–496

**Hassidim M, Keren N, Ohad I, Reinhold L, Kaplan A** (1997) Acclimation of *Synechococcus* strain WH7803 to ambient $CO_2$ concentration and to elevated light intensity. J Phycol **33:** 811–817

**Hopkinson BM** (2014) A chloroplast pump model for the $CO_2$ concentrating mechanism in the diatom *Phaeodactylum tricornutum*. Photosynth Res **121:** 223–233

**Hopkinson BM, Barbeau KA** (2012) Iron transporters in marine prokaryotic genomes and metagenomes. Environ Microbiol **14:** 114–128

**Hopkinson BM, Dupont CL, Allen AE, Morel FMM** (2011) Efficiency of the $CO_2$-concentrating mechanism of diatoms. Proc Natl Acad Sci USA **108:** 3830–3837

**Johnson KS** (1982) Carbon dioxide hydration and dehydration kinetics in seawater. Limnol Oceanogr **27:** 849–855

**Kallas T, Dahlquist FW** (1981) Phosphorus-31 nuclear magnetic resonance analysis of internal pH during photosynthesis in the cyanobacterium Synechococcus. Biochemistry **20:** 5900–5907

**Kaplan A, Badger MR, Berry JA** (1980) Photosynthesis and the intracellular inorganic carbon pool in the bluegreen alga *Anabaena variabilis*: response to external $CO_2$ concentration. Planta **149:** 219–226

**Kettler GC, Martiny AC, Huang K, Zucker J, Coleman ML, Rodrigue S, Chen F, Lapidus A, Ferriera S, Johnson J, et al** (2007) Patterns and implications of gene gain and loss in the evolution of *Prochlorococcus*. PLoS Genet **3:** e231

**Kinney JN, Axen SD, Kerfeld CA** (2011) Comparative analysis of carboxysome shell proteins. Photosynth Res **109:** 21–32

**Klein MG, Zwart P, Bagby SC, Cai F, Chisholm SW, Heinhorst S, Cannon GC, Kerfeld CA** (2009) Identification and structural analysis of a novel carboxysome shell protein with implications for metabolite transport. J Mol Biol **392:** 319–333

**Losh JL, Young JN, Morel FM** (2013) Rubisco is a small fraction of total protein in marine phytoplankton. New Phytol **198:** 52–58

**Maeda S, Badger MR, Price GD** (2002) Novel gene products associated with NdhD3/D4-containing NDH-1 complexes are involved in photosynthetic $CO_2$ hydration in the cyanobacterium, *Synechococcus* sp. PCC7942. Mol Microbiol **43:** 425–435

**Martiny AC, Kathuria S, Berube PM** (2009) Widespread metabolic potential for nitrite and nitrate assimilation among *Prochlorococcus* ecotypes. Proc Natl Acad Sci USA **106:** 10787–10792

**Matsuda Y, Nakajima K, Tachibana M** (2011) Recent progresses on the genetic basis of the regulation of $CO_2$ acquisition systems in response to $CO_2$ concentration. Photosynth Res **109:** 191–203

**Menon BB, Heinhorst S, Shively JM, Cannon GC** (2010) The carboxysome shell is permeable to protons. J Bacteriol **192:** 5881–5886

**Moore L, Coe A, Zinser E, Saito M, Sullivan M, Lindell D, Frois-Moniz K, Waterbury J, Chisholm S** (2007) Culturing the marine cyanobacterium *Prochlorococcus*. Limnol Oceanogr Methods **5:** 353–362

**Morris JJ, Johnson ZI, Szul MJ, Keller M, Zinser ER** (2011) Dependence of the cyanobacterium *Prochlorococcus* on hydrogen peroxide scavenging microbes for growth at the ocean's surface. PLoS ONE **6:** e16805

**Nishimura T, Takahashi Y, Yamaguchi O, Suzuki H, Maeda S, Omata T** (2008) Mechanism of low $CO_2$-induced activation of the cmp bicarbonate transporter operon by a LysR family protein in the cyanobacterium *Synechococcus elongatus* strain PCC 7942. Mol Microbiol **68:** 98–109

**Ogawa T, Mi H** (2007) Cyanobacterial NADPH dehydrogenase complexes. Photosynth Res **93:** 69–77

**Omata T, Gohta S, Takahashi Y, Harano Y, Maeda S** (2001) Involvement of a CbbR homolog in low $CO_2$-induced activation of the bicarbonate transporter operon in cyanobacteria. J Bacteriol **183:** 1891–1898

**Palinska KA, Laloui W, Bédu S, Loiseaux-de Goër S, Castets AM, Rippka R, Tandeau de Marsac N** (2002) The signal transducer $P_{II}$ and bicarbonate acquisition in *Prochlorococcus marinus* PCC 9511, a marine cyanobacterium naturally deficient in nitrate and nitrite assimilation. Microbiology **148:** 2405–2412

**Partensky F, Garczarek L** (2010) Prochlorococcus: advantages and limits of minimalism. Annu Rev Mar Sci **2:** 305–331

**Partensky F, Hess WR, Vaulot D** (1999) *Prochlorococcus*, a marine photosynthetic prokaryote of global significance. Microbiol Mol Biol Rev **63:** 106–127

**Pasciak WJ, Gavis J** (1974) Transport limitation of nutrient uptake in phytoplankton. Limnol Oceanogr **19:** 881–898

**Price GD, Badger MR** (1989) Expression of human carbonic anhydrase in the cyanobacterium *Synechococcus* PCC7942 creates a high $CO_2$-requiring phenotype: evidence for a central role for carboxysomes in the $CO_2$ concentrating mechanism. Plant Physiol **91:** 505–513

**Price GD, Woodger FJ, Badger MR, Howitt SM, Tucker L** (2004) Identification of a SulP-type bicarbonate transporter in marine cyanobacteria. Proc Natl Acad Sci USA **101:** 18228–18233

**Rae BD, Förster B, Badger MR, Price GD** (2011) The $CO_2$-concentrating mechanism of *Synechococcus* WH5701 is composed of native and horizontally-acquired components. Photosynth Res **109:** 59–72

**Rae BD, Long BM, Badger MR, Price GD** (2013) Functions, compositions, and evolution of the two types of carboxysomes: polyhedral microcompartments that facilitate $CO_2$ fixation in cyanobacteria and some proteobacteria. Microbiol Mol Biol Rev **77:** 357–379

**Reinhold L, Kosloff R, Kaplan A** (1991) A model for inorganic carbon fluxes and photosynthesis in cyanobacterial carboxysomes. Can J Bot **69:** 984–988

**Reinhold L, Zviman M, Kaplan A** (1987) Inorganic carbon fluxes and photosynthesis in cyanobacteria: a quantitative model *In* **J Biggins**, ed,

Progress in Photosynthesis. Martinus Nijhoff, Dordrecht, The Netherlands, pp 289–296

**Roberts EW, Cai F, Kerfeld CA, Cannon GC, Heinhorst S** (2012) Isolation and characterization of the *Prochlorococcus* carboxysome reveal the presence of the novel shell protein CsoS1D. J Bacteriol **194:** 787–795

**Rocap G, Larimer FW, Lamerdin J, Malfatti S, Chain P, Ahlgren NA, Arellano A, Coleman M, Hauser L, Hess WR, et al** (2003) Genome divergence in two *Prochlorococcus* ecotypes reflects oceanic niche differentiation. Nature **424:** 1042–1047

**Rost B, Riebesell U, Burkhardt S, Sültemeyer D** (2003) Carbon acquisition of bloom-forming marine phytoplankton. Limnol Oceanogr **48:** 55–67

**Rost B, Zondervan I, Wolf-Gladrow D** (2008) Sensitivity of phytoplankton to future changes in ocean carbonate chemistry: current knowledge, contradictions and research directions. Mar Ecol Prog Ser **373:** 227–237

**Rusch DB, Martiny AC, Dupont CL, Halpern AL, Venter JC** (2010) Characterization of *Prochlorococcus* clades from iron-depleted oceanic regions. Proc Natl Acad Sci USA **107:** 16184–16189

**Scott KM, Henn-Sax M, Harmer TL, Longo DL, Framer CH, Cavanaugh CM** (2007) Kinetic isotope effect and biochemical characterization of form IA RubisCO from the marine cyanobacterium *Prochlorococcus marinus* MIT9313. Limnol Oceanogr **52:** 2199–2204

**Shibata M, Katoh H, Sonoda M, Ohkawa H, Shimoyama M, Fukuzawa H, Kaplan A, Ogawa T** (2002) Genes essential to sodium-dependent bicarbonate transport in cyanobacteria: function and phylogenetic analysis. J Biol Chem **277:** 18658–18664

**Shibata M, Ohkawa H, Kaneko T, Fukuzawa H, Tabata S, Kaplan A, Ogawa T** (2001) Distinct constitutive and low-$CO_2$-induced $CO_2$ uptake systems in cyanobacteria: genes involved and their phylogenetic relationship with homologous genes in other organisms. Proc Natl Acad Sci USA **98:** 11789–11794

**Silverman DN, Tu CK, Roessler N** (1981) Diffusion-limited exchange of $^{18}O$ between $CO_2$ and water in red cell suspensions. Respir Physiol **44:** 285–298

**So AKC, Espie GS, Williams EB, Shively JM, Heinhorst S, Cannon GC** (2004) A novel evolutionary lineage of carbonic anhydrase (epsilon class) is a component of the carboxysome shell. J Bacteriol **186:** 623–630

**Tcherkez GGB, Farquhar GD, Andrews TJ** (2006) Despite slow catalysis and confused substrate specificity, all ribulose bisphosphate carboxylases may be nearly perfectly optimized. Proc Natl Acad Sci USA **103:** 7246–7251

**Tchernov D, Hassidim M, Luz B, Sukenik A, Reinhold L, Kaplan A** (1997) Sustained net $CO_2$ evolution during photosynthesis by marine microorganisms. Curr Biol **7:** 723–728

**Ting CS, Hsieh C, Sundararaman S, Mannella C, Marko M** (2007) Cryoelectron tomography reveals the comparative three-dimensional architecture of *Prochlorococcus*, a globally important marine cyanobacterium. J Bacteriol **189:** 4485–4493

**Tolonen AC, Aach J, Lindell D, Johnson ZI, Rector T, Steen R, Church GM, Chisholm SW** (2006) Global gene expression of *Prochlorococcus* ecotypes in response to changes in nitrogen availability. Mol Syst Biol **2:** 53

**Whitehead L, Long BM, Price GD, Badger MR** (2014) Comparing the in vivo function of $\alpha$-carboxysomes and $\beta$-carboxysomes in two model cyanobacteria. Plant Physiol **165:** 398–411

**Woodger FJ, Badger MR, Price GD** (2005) Sensing of inorganic carbon limitation in *Synechococcus* PCC7942 is correlated with the size of the internal inorganic carbon pool and involves oxygen. Plant Physiol **139:** 1959–1969

**Woodger FJ, Bryant DA, Price GD** (2007) Transcriptional regulation of the $CO_2$-concentrating mechanism in a euryhaline, coastal marine cyanobacterium, *Synechococcus* sp. strain PCC 7002: role of NdhR/CcmR. J Bacteriol **189:** 3335–3347

**Worden AZ, Binder BJ** (2003) Application of dilution experiments for measuring growth and mortality rates among *Prochlorococcus* and *Synechococcus* populations in oligotrophic environments. Aquat Microb Ecol **30:** 159–174

**Zeebe RE, Wolf-Gladrow D** (2001) $CO_2$ in Seawater: Equilibrium, Kinetics, Isotopes. Elsevier, Amsterdam

**Zhang HN, Byrne RH** (1996) Spectrophotometric pH measurements of surface seawater at in-situ conditions: absorbance and protonation behavior of thymol blue. Mar Chem **52:** 17–25